24th COBEM - 2017

24th ABCM International Congress of Mechanical Engineering
December 3-8, 2017, Curitiba, PR, Brazil

COBEM-2017-1627
EVALUATION OF THE EFFECT OF OZONE ADDITION ON THE METHANE/OXYGEN COMBUSTION IN A LPRE USING CFD ANALYSIS

Francisco de Souza Forte Neto
Rene Francisco Boschi Gonçalves
Universidade Federal do Pará, Rua Augusto Corrêa, 01. Belém, PA. Brasil
Instituto Tecnológico de Aeronáutica, Praça Marechal Eduardo Gomes, 50. São José dos Campos
fforteneto@gmail.com
renefbg@ita.com

Abstract. *In the present work the methane/oxygen combustion process is analyzed in the combustion chamber of a conventional liquid propellant rocket engine (LPRE), using ozone as a process enriching species in order to verify the viability or not of its use in propulsive systems. For this study, simulations were carried out using the ANSYS Fluent 16.2 software package, coupled with a detailed reaction mechanism for the combustion of methane/oxygen/ozone imported from the CHEMKIN software, in order to capture its effect on combustion and bring the results as close to reality as possible. Through this work, was possible to verify that ozone has indeed enriching potential in the combustion of methane/oxygen, generating increases of about 100K in the temperature of the chamber, which can lead to lower fuel consumption.*

Keywords: *Combustion, ozone, methane/oxygen, liquid propellant, ANSYS Fluent.*

1. INTRODUCTION

Conventional rockets operate according to the principle of Newton's third law, where all action causes an opposite reaction of the same direction and magnitude, in the liquid propellant engines this action is caused by the gases resulting from the combustion that occurred inside the chamber, which are released to the atmosphere resulting in an opposing force that is responsible for propel the rocket.

For systems that have their operation based on the use of the energy coming from the combustion process, is very important understand and improve this process, for that reason, the study of the effects caused by the enrichment of the combustion is an area that has been the focus of research in recent years, especially in internal combustion engines.

Liquid ozone has a great potential to be used as an oxidizer in rocket engines, but its use was greatly discouraged because of its strong tendency to propagate destructive detonations (MILLER, 1958; MILLER & BROWN, 1959). Studies indicate that at concentrations of ozone in oxygen below 35% can be safe, not propagating strong explosions in half-inch tubes (MILLER, 1958).

In the last times, the increasing need to reduce costs, time and increase the quality of propulsive systems, allied with the advances in computational codes of fluid dynamics, has promoted the use of computational simulation to perform qualitative and quantitative analysis of propulsive systems, which considerably reduces the costs that would be used in apparatus for experimental analysis.

2. COMPUTATIONAL PROCEDURE

The simulation was performed in the ANSYS Fluent 16.2 software package, the present software uses the finite volume method to solve the equations that rules the dynamic behavior of the fluids, also describing flows in which the involved species react with each other, allowing the implementation of reactional mechanisms that can be imported from other software such as CHEMKIN.

2.1 Geometry and Mesh

The first step taken to start the simulation, just after the choice of the case to be simulated, was the creation of geometry. For the creation of the geometry, the drawing tool present in ANSYS WORKBENCH 16.2 (DesignModeler) was used. The dimensions adopted for the combustion chamber were one meter in length (to allow a better visualization

of the development of the flame inside the chamber) and five inches in diameter or 0,127 meters (due to the geometry of the nozzle used). The geometry of the nozzle chosen for the rocket motor was taken from the work of Back *et al.* (1965) of a team of JPL (Jet Propulsion Laboratory) of NASA (National Aeronautics and Space Administration). To analyze the behavior of the flow after its passage through the nozzle, a control region corresponding to the external ambient with 0.60 m x 0.35 m was created, as shown in Fig. 1.

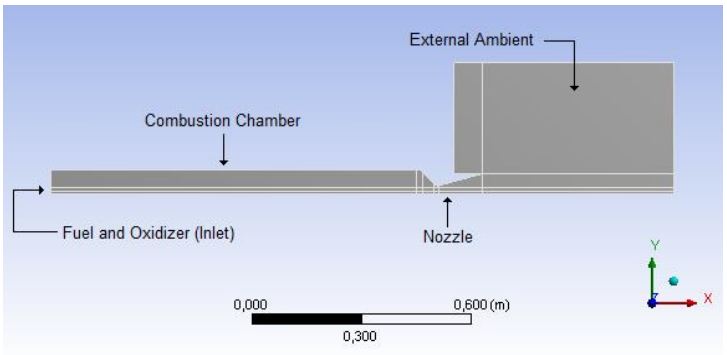

Figure 1. Geometry created in the software.

In order to use the created geometry as a control volume, it is necessary to create a mesh that will discretize the domain, enabling the solution of the equations of government in numerical form. The mesh is a very important element of the simulation, has direct influence in the convergence and precision of the results.

To generate the mesh, was used the mesh generator present in the ANSYS WORKBENCH 16.2 (Meshing). The mesh was created entirely with rectangular elements, as can be observed in Fig. 2, with a total of 20660 elements and 21483 nodes. In its creation process, it was tried to use smaller elements in the regions of greater interest, with the intention of increasing the accuracy of the results in these places.

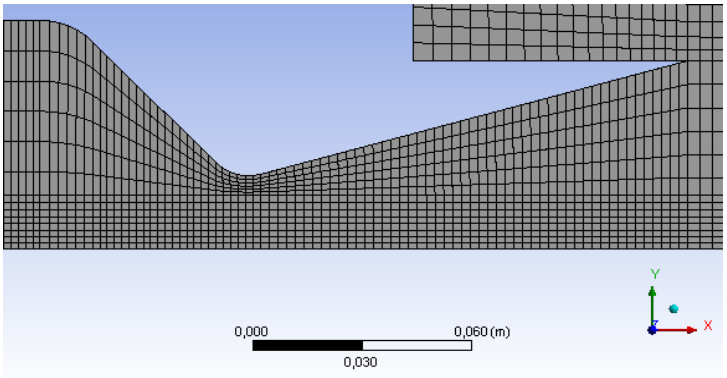

Figure 2. Mesh in the nozzle region.

2.2 Reaction mechanism

In order to capture more accurately the effects of the addition of ozone in the combustion process, it was added to the methane oxidation mechanism proposed by Tianfeng et al. (2008), which consists of a skeletal mechanism of 30 species, the ozone reactions. The mechanism used in the ozone modeling and the Arrhenius data of each elemental reaction are listed in the table below.

Table 1. Ozone combustion mechanism.

Reactions	A (mol-cm-s-K)	b	E (cal/mol)
O3+H=O2+OH	1,64E+13	0,8	750,0
O3+H=O+HO2	4,52E+11	0,0	0,0
O3+OH=O2+HO2	1,15E+12	0,0	1990,0
O3+H2O=O2+H2O2	6,62E+01	0,0	0,0
O3+HO2=2O2+OH	1,19E+08	4,6	1380,0
O3+CO=O2+CO2	6,02E+02	0,0	0,0

O3+N=O2+NO	6,00E+07	0,0	0,0
O3+NO=NO2+O2	8,43E+11	0,0	2600,0
O3+NO2=O2+NO3	8,43E+10	0,0	4870,0
O2+O=O3	4,86E+13	-1,0	0,0
O3+O=2O2	4,82E+12	0,0	4090,0

2.3 Modeling

The proposed system was discretized in the form of an axisymmetric reactive flow where the fuel and the oxidant are injected into the combustion chamber through concentric inputs. For the modeling of the combustion process, it was adopted the non-premixed combustion model that is available in the ANSYS Fluent 16.2 package. The geometric parameters as well as the input values for the system were defined based on a correlation made with the parameters adopted by Phing, (2008). For the description of the flow turbulence, the standard κ-ε turbulence model was adopted.

Table 2. Simulation input parameters.

Equivalence Ratio	0,30
Fuel Mass Flow	0,015 kg/s
Oxidant Mass Flow	0,200 kg/s
Fuel Temperature	300 K
Oxidant Temperature	300 K

To determine the percentages of ozone to be studied in the simulation, a literature search was carried out, where it was verified that large amounts of ozone are not viable, as it has a strong tendency to propagate detonations, as mentioned by Miller et al., (1959). Another limiting factor was the fact that the model did not converge, even after several iterations, to large percentages of the additive, due to the more complex the balance of the species, especially for the simulations that were performed with the detailed kinetic model. In this work, the effects of ozone are analyzed in a range of 0 to 8% in mass fraction of the oxidant.

3. RESULTS AND DISCUSSION

First, the results obtained in the simulations performed with and without the detailed kinetic mechanism for 0% of ozone will be compared, after that the simulation results performed with the mechanism for a range of 0% to 8% ozone in a mass fraction of the oxidant will be presented.

3.1 Simulations with and without reaction mechanism

In this section the results of the simulations are presented below, where the temperature, pressure, velocity and mass fraction contours of the combustion products are compared.

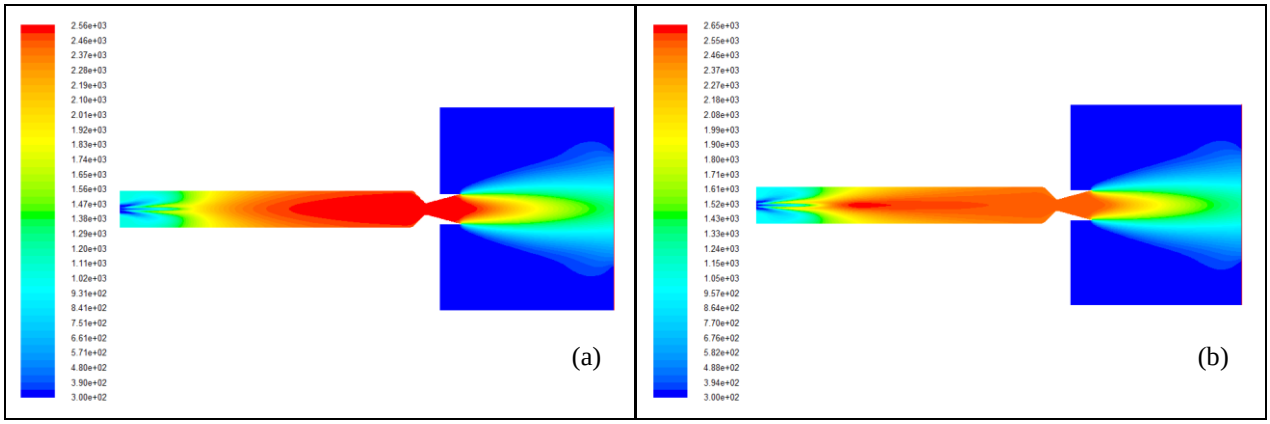

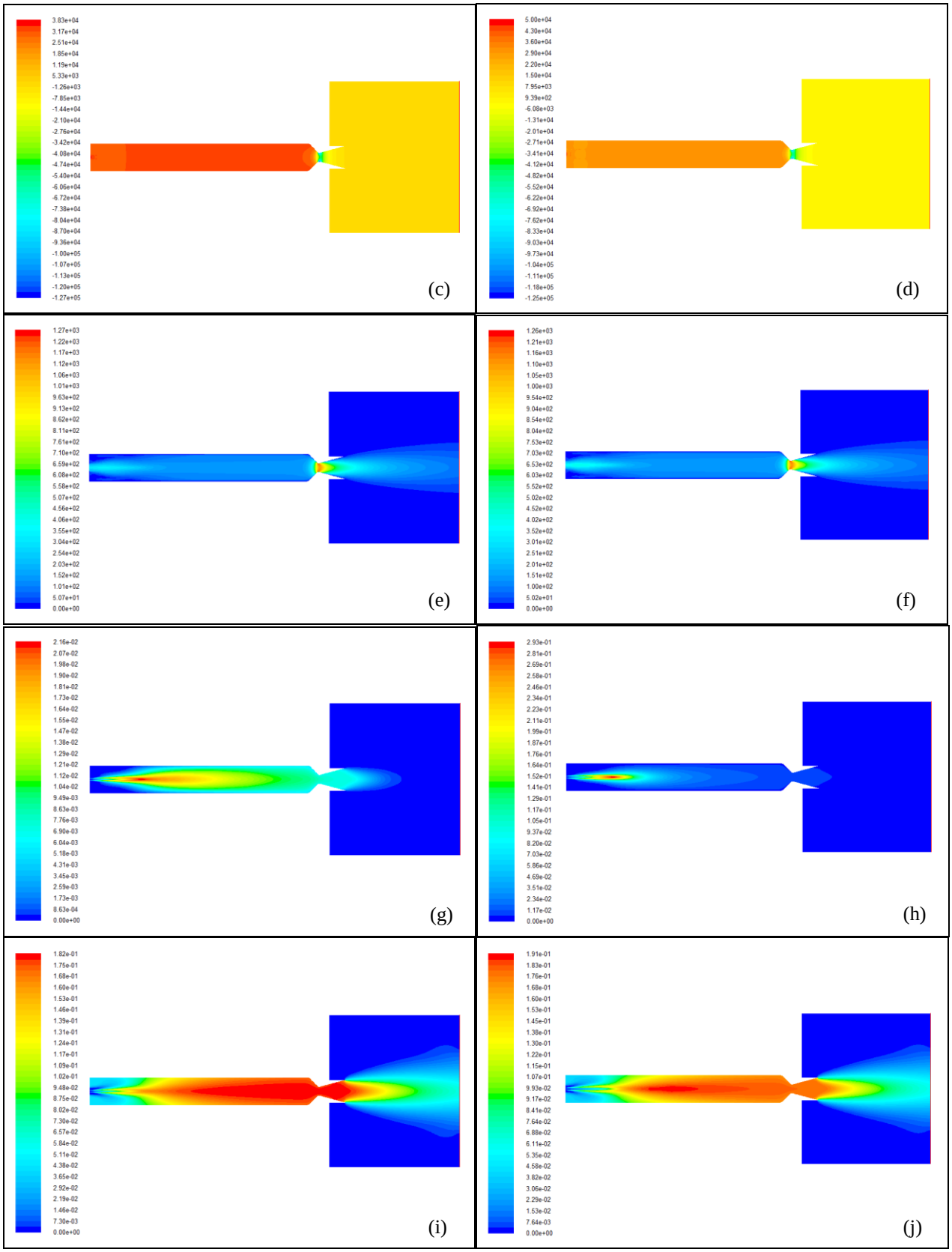
3.83e+04
3.17e+04
2.51e+04
1.85e+04
1.19e+04
5.33e+03
-1.26e+03
-7.85e+03
-1.44e+04
-2.10e+04
-2.76e+04
-3.42e+04
-4.08e+04
-4.74e+04
-5.40e+04
-6.06e+04
-6.72e+04
-7.38e+04
-8.04e+04
-8.70e+04
-9.36e+04
-1.00e+05
-1.07e+05
-1.13e+05
-1.20e+05
-1.27e+05
(c)
5.00e+04
4.30e+04
3.60e+04
2.90e+04
2.20e+04
1.50e+04
7.95e+03
9.39e+02
-6.08e+03
-1.31e+04
-2.01e+04
-2.71e+04
-3.41e+04
-4.12e+04
-4.82e+04
-5.52e+04
-6.22e+04
-6.92e+04
-7.62e+04
-8.33e+04
-9.03e+04
-9.73e+04
-1.04e+05
-1.11e+05
-1.18e+05
-1.25e+05
(d)
1.27e+03
1.22e+03
1.17e+03
1.12e+03
1.06e+03
1.01e+03
9.63e+02
9.13e+02
8.62e+02
8.11e+02
7.61e+02
7.10e+02
6.59e+02
6.08e+02
5.58e+02
5.07e+02
4.56e+02
4.06e+02
3.55e+02
3.04e+02
2.54e+02
2.03e+02
1.52e+02
1.01e+02
5.07e+01
0.00e+00
(e)
1.26e+03
1.21e+03
1.16e+03
1.10e+03
1.05e+03
1.00e+03
9.54e+02
9.04e+02
8.54e+02
8.04e+02
7.53e+02
7.03e+02
6.53e+02
6.03e+02
5.52e+02
5.02e+02
4.52e+02
4.02e+02
3.52e+02
3.01e+02
2.51e+02
2.01e+02
1.51e+02
1.00e+02
5.02e+01
0.00e+00
(f)
2.16e-02
2.07e-02
1.98e-02
1.90e-02
1.81e-02
1.73e-02
1.64e-02
1.55e-02
1.47e-02
1.38e-02
1.29e-02
1.21e-02
1.12e-02
1.04e-02
9.49e-03
8.63e-03
7.76e-03
6.90e-03
6.04e-03
5.18e-03
4.31e-03
3.45e-03
2.59e-03
1.73e-03
8.63e-04
0.00e+00
(g)
2.93e-01
2.81e-01
2.69e-01
2.58e-01
2.46e-01
2.34e-01
2.23e-01
2.11e-01
1.99e-01
1.87e-01
1.76e-01
1.64e-01
1.52e-01
1.41e-01
1.29e-01
1.17e-01
1.05e-01
9.37e-02
8.20e-02
7.03e-02
5.86e-02
4.69e-02
3.51e-02
2.34e-02
1.17e-02
0.00e+00
(h)
1.82e-01
1.75e-01
1.68e-01
1.60e-01
1.53e-01
1.46e-01
1.39e-01
1.31e-01
1.24e-01
1.17e-01
1.09e-01
1.02e-01
9.48e-02
8.75e-02
8.02e-02
7.30e-02
6.57e-02
5.84e-02
5.11e-02
4.38e-02
3.65e-02
2.92e-02
2.19e-02
1.46e-02
7.30e-03
0.00e+00
(i)
1.91e-01
1.83e-01
1.76e-01
1.68e-01
1.60e-01
1.53e-01
1.45e-01
1.38e-01
1.30e-01
1.22e-01
1.15e-01
1.07e-01
9.93e-02
9.17e-02
8.41e-02
7.64e-02
6.88e-02
6.11e-02
5.35e-02
4.58e-02
3.82e-02
3.06e-02
2.29e-02
1.53e-02
7.64e-03
0.00e+00
(j)

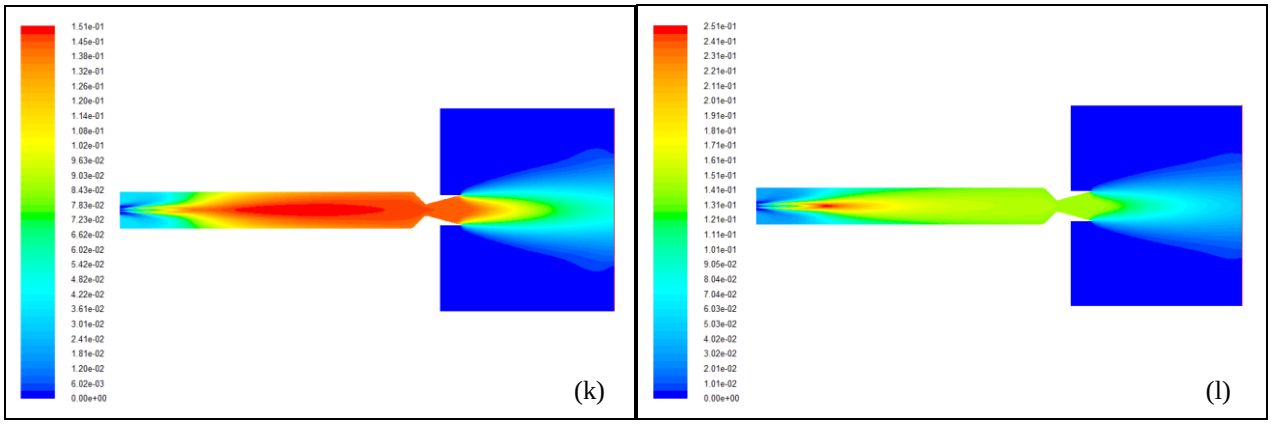

Figure 3. Comparison between the contours of temperature (K), pressure (Pa), velocity (m/s), mass fraction of CO, CO_2 and H_2O, respectively, at 0% of ozone. Simulation with global reaction in the left and with detailed kinetics in the right.

From the contours shown in Fig. 3 it is possible to notice a series of differences between the results obtained in the simulations with and without the reaction mechanism. With the addition of the mechanism, there is a smoother temperature dissipation inside the chamber diverging from the temperature distribution found in the simulation without the mechanism, Fig. 3 (a) and (b) where there is a large region where the maximum temperature is concentrated. In the pressure contours Fig. 3 (c) and (d), as well as in the speed contours (e) and (f), there were no large changes in the contours, only a small increase in the maximum speed and an increase in the system pressure. The contours of the mass fractions of CO, CO_2 and H_2O (g) to (1), respectively, as expected due to the implementation of the kinetic model, were the ones that presented the greatest variations of the results. As it can be observed, CO is mostly consumed inside the combustion chamber, the CO_2 profile suffer a similar change that occurred in the temperature profile, with a higher concentration of the species inside the chamber and the H_2O profile presented an increase in the values of the mass fraction in all the contour.

It is also verified that the input parameters used generated a very efficient internal combustion in the rocket engine, since the presence of the flame still inside the combustion chamber, with few areas of recirculation and significant increase of the temperature. At the exit of the nozzle there is still a certain pressure difference with the external atmosphere, generating variation in the exhaust plume, which can cause a reduction of the specific impulse of the engine.

3.2 Simulation with the addition of ozone

In this section the results of the simulations with the detailed kinetic mechanism are presented below, where the temperature contours, mass fraction of the combustion products and velocity profiles at the nozzle outlet are compared for different ozone concentrations in the oxidant.

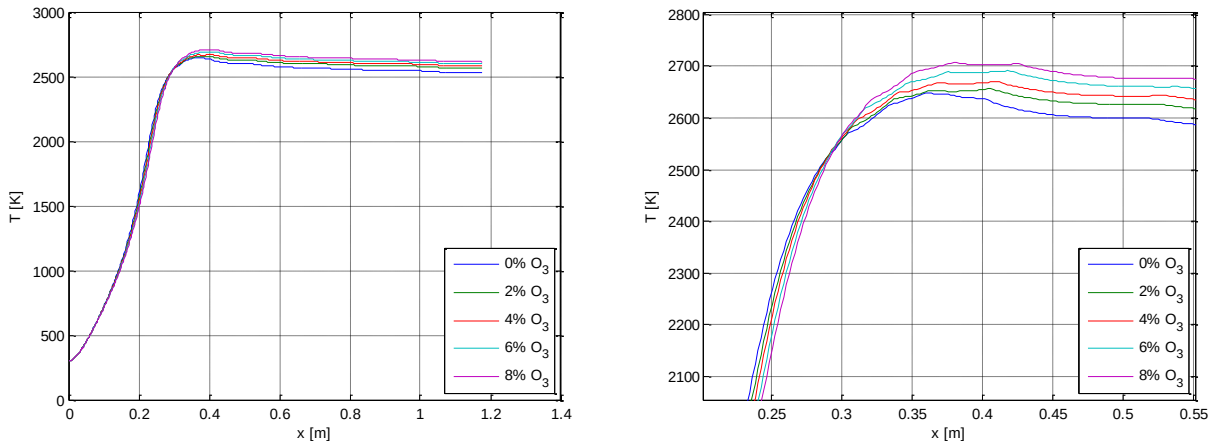

Figure 4. Temperature distribution along the rocket engine (enlargement of the left-hand chart in the right-hand image).

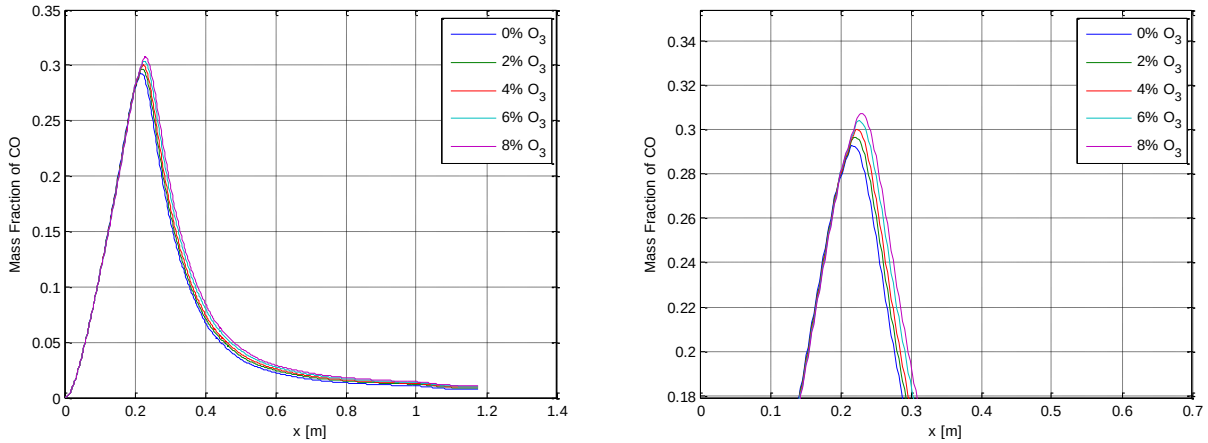

Figure 5. Distribution of CO along the rocket engine (enlargement of the left-hand chart in the right-hand image).

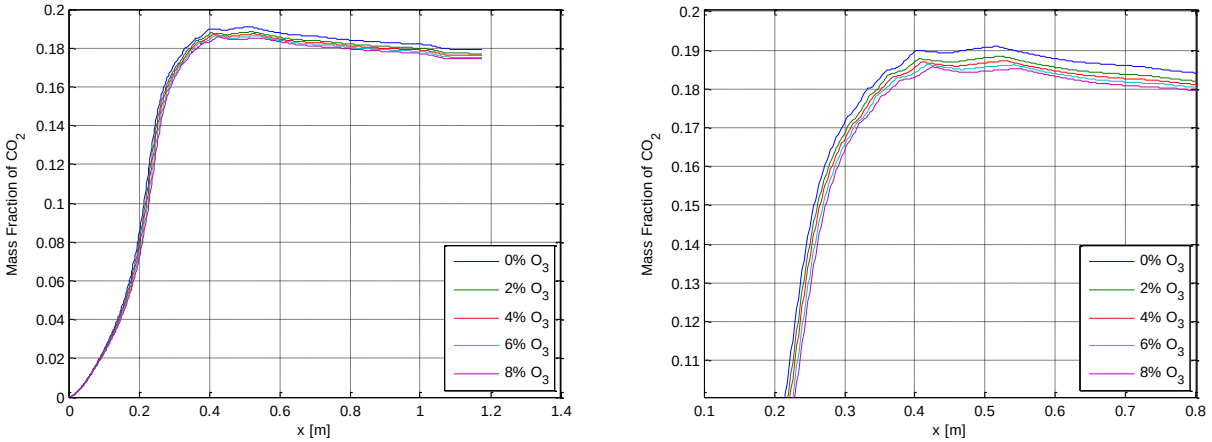

Figure 6. CO_2 distribution along the rocket engine (enlargement of the left-hand chart in the right-hand image).

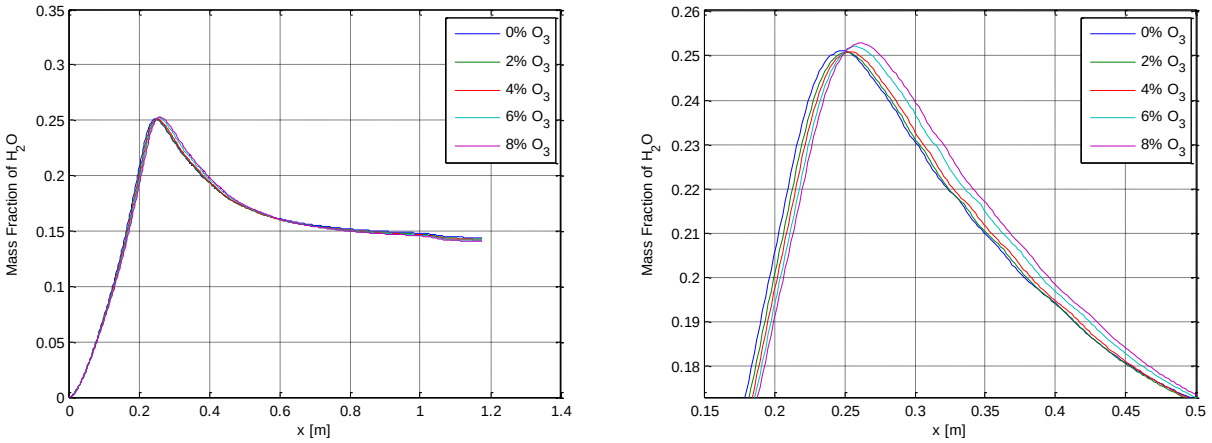

Figure 7. Distribution of H_2O along the rocket engine (enlargement of the left-hand chart in the right-hand image).

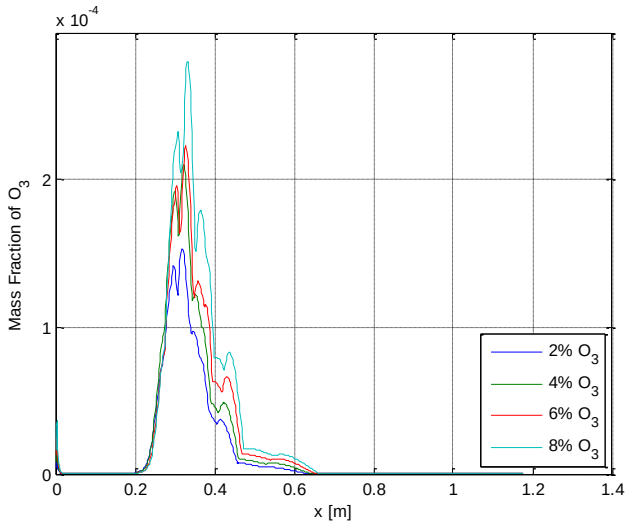

Figure 8. Distribution of O_3 along the rocket engine.

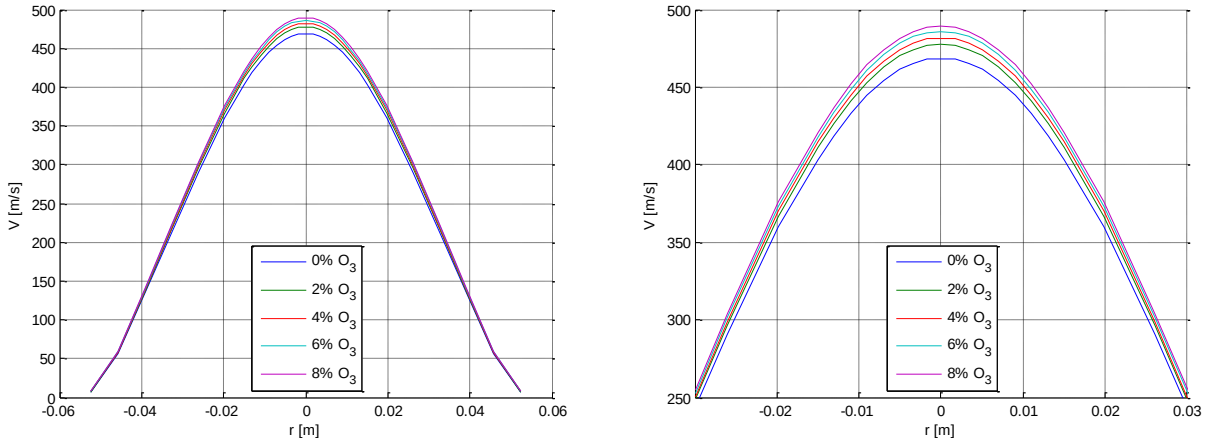

Figure 9. Velocity profiles at the nozzle outlet (enlargement of the left-hand chart in the right-hand image).

As shown in Fig. 4, in the zone corresponding to the interior of the combustion chamber it is possible to be noticed that there are small elevations in the maximum temperature within the rocket engine. Ozone can therefore allow a reduction in the specific consumption of the system, allowing the rocket engine to reach greater distances (or impulse).

In the graphs of the distribution of the mass fraction of the combustion products (Fig. 5-7), it can be observed that for both CO and H_2O there is an increase in the concentration of these species as the concentration of ozone increases, whereas for CO_2, the process occurs inversely, with a reduction in its concentration. These variations in species concentrations are due to the large amount of radicals released by ozone during the combustion process, which turns combustion into a radical process.

In Fig. 8 it is observed that the ozone is totally consumed during the combustion process, still inside the combustion chamber near the injection site.

In Fig. 9, it is possible to note that there are increases in velocity at the outlet of the nozzle as the percentage of ozone increases. This growth may mean a rise in the propulsive systems' specific impulse due to the increased exhaust velocity of the combustion gases.

4. CONCLUSIONS

In the present work the combustion of methane/oxygen was analyzed in the combustion chamber of a rocket engine with a conventional liquid propellant, in which the ozone was added in order to verify its influence in this process by means of computational simulations. As can be verified, ozone has characteristics that are enriching for the methane/oxygen combustion process, however, this influence presented in this simulation was smaller than expected, but still significant, as the temperature developed inside the system was raised for about 100 K with 8% of ozone in the

injection mixture. This increase may lead to the activation of other elementary reactions, leading to lower fuel consumption and higher efficiency during the operation of the rocket. It is important to point out that the small influence presented by ozone in this simulation requires yet experimental analysis and for its use are necessary evaluations of the metallurgical and ballistic effects in the system and structure of the rocket, in function of its high reactivity and oxidizing power.

5. ACKNOWLEDGEMENTS

The authors thank FAPESPA for the financial support rendered.

6. REFERENCES

BACK, L. H., MASSIER P. F., GIER H. L., Comparison of measured and predicted flows through conical supersonic nozzles with emphasis on transonic region, AIAA Journal, vol. 3, pp. 1606–1614, 1965.

MILLER, R., BROWN, D., Effect of Ozone Addition on Combustion Efficiency of Hydrogen - Liquid-Oxygen Propellant in Small Rockets, Lewis Research Center, NASA, Cleveland, Ohio. 1959.

MILLER, R., Detonation Propagation in Liquid Ozone-Oxyge, Lewis Research Center, NASA, Cleveland, Ohio. 1958.

PHING, A. Simulating Combustion Flow in a Rocket Chamber. 2008. 41p. Master Thesis – Luleå University of Technology, Departament of Space Science, Kiruana. 2008.

TIANFENG LU, CHUNG K. LAW, A criterion based on computational singular perturbation for the identification of quasi steady state species: A reduced mechanism for methane oxidation with NO chemistry, Combustion and Flame, Vol.154 No.4 pp.761–774, 2008.

7. RESPONSIBILITY NOTICE

The authors are the only responsible for the printed material included in this paper.